

# Measurements of K X-ray fluorescence cross-sections, fluorescence yields, level widths and radiative vacancy transition probabilities for the elements Zr, Mo, Cd, Er at 59.54 keV

Mehmet Fatih Turhan<sup>1</sup>, Ferdi Akman<sup>2,\*</sup>, Mustafa Recep Kaçal<sup>3</sup> and Rıdvan Durak<sup>4</sup>

<sup>1</sup>Afyon Kocatepe University, Ataturk Vocational School of Health Services, Medical Imaging Techniques, 03200 Afyonkarahisar, Turkey.

<sup>2</sup>Bingol University, Vocational School of Technical Sciences, Department of Electronic Communication Technology, 12000 Bingol, Turkey.

<sup>3</sup>Giresun University, Arts and Sciences Faculty, Department of Physics, 28100 Giresun, Turkey. Afyon Kocatepe

<sup>4</sup>Ataturk University, Sciences Faculty, Department of Physics, 25240 Erzurum, Turkey.

\*Corresponding Author: fakman@bingol.edu.tr

**Abstract.** K shell X ray fluorescence cross sections, fluorescence yields, level widths and radiative vacancy transition probabilities were investigated for the elements Zr, Mo, Cd, Er. The measurements were performed using photons of 59.54 keV emitted from an Am-241 (about 100 mCi) point source and a high resolution Si(Li) detector. The experimental results were compared with theoretical calculations and the other results obtained from literature.

## 1. Introduction

One of the techniques used worldwide in many fields of science is energy dispersive X-ray fluorescence technique because EDXRF is comparatively low-cost and requires less technical effort to run the system. This technique is very useful for determining physical parameters such as fluorescence cross sections, fluorescence yields, level widths and vacancy transfer probabilities, intensity ratios, etc. The knowledge obtained from these physical parameters for different elements, compounds, polymers, thin films, ores, food productions, ceramics is very important in the study of some basic phenomena such as atomic, molecular and radiation physics, medical physics, environmental science, agriculture, nuclear science, trace element analysis, etc.

Several investigators determined the X-ray fluorescence cross sections, fluorescence yields, level widths, intensity ratios [1-19]. The semi-empirically fitted values of K shell X-ray fluorescence, auger



and Coster–Kronig transition probabilities for all elements in the atomic number range  $5 \leq Z \leq 110$  were determined by Krause, [1]. K and L X ray fluorescence cross sections and fluorescence yields for some elements in the atomic range  $22 \leq Z \leq 50$  at 59,54 keV incidents photon were investigated by Yilmaz et al., [2], Şimşek et al. [3], Durak et al. [4], Han et al. [5], Akman et al. [6]. Gudennavar et al. [7], Durak [8] measured K-shell fluorescence yield, fluorescence cross-section and ratio between the radiative transition width and the Auger transition width for some elements in the atomic range from  $30 \leq Z \leq 70$  at 123,6 keV incidents photon. Krause and Oliver [9] presented the semi-empirical values of the natural widths of the K,  $L_1$ ,  $L_2$  and  $L_3$  levels,  $K_{\alpha 1}$ ,  $K_{\alpha 2}$  X-ray lines and  $KL_1L_1$ ,  $KL_1L_2$  and  $KL_2L_3$  auger lines for the elements  $10 \leq Z \leq 110$ . Campbell and Papp [10] combined atomic level widths from experimental measurements and they calculated theoretical widths based upon the Dirac-Hartree-Slater version of the independent particle model. K shell intensity ratios, production cross sections, fluorescence yields, vacancy transfer probabilities from K to L shell, level widths and line widths for some heavy elements in the atomic range  $73 \leq Z \leq 81$  were measured by Cengiz et al. [11]. Ertugrul [12] measured fluorescence yields and level widths of some atomic sub-shells for Th and U using measurements of the L X-ray from targets. Ertuğrul [13] evaluated K shell radiative transition probabilities and K,  $L_2$  and  $L_3$  shell/subshell fluorescence yields for Zn, As, Se, Rb, Sr, Y and Zr. The K to Li ( $i=2, 3$ ), K to L, and K to M shell vacancy transfer probabilities for La, Ce, Pr, Nd, Sm, Eu, Gd, Tb, Dy and Er were determined at 59.54 keV using a reflection geometry by Akman [14]. Bennal et al. [15] determined the K-L total vacancy transfer probabilities ( $\eta_{KL}$ ) of selected elements in the atomic range  $42 \leq Z \leq 82$  using a weak gamma source. Using the intensity ratios, the radiative vacancy transfer probabilities from the shell K to the L sub-shells for selected rare earth were determined by Herrera and Miranda [16]. Bonzi [17] investigated the the radiative vacancy transfer probabilities from  $L_3$  to M shell and  $L_3$  to N shell for W, Re and Pb. Vacancy transfer probabilities from  $L_3$  sub-shell to M, N and O shells and sub-shells for the elements Hf, Ta, W, Re, Pt, Au, HgO, Tl, Pb, Bi, Th, U were measured using L shell fluorescence yields and X-ray intensity ratios by Tuzluca et al. [18]. Turhan et al. [19] investigated L X-ray fluorescence cross sections, L sub-shell fluorescence yields, level widths and radiative vacancy transfer probabilities of L sub-shells to  $M_i$ ,  $N_i$  and  $O_i$  sub-shells for the elements Ho, Lu, W, Hg and Bi.

In this study, we determined K shell fluorescence cross sections, fluorescence yields, level widths and K to  $L_2$ ,  $L_3$ ,  $M_2$ ,  $M_3$  radiative vacancy transfer probabilities for Zr, Mo, Cd, Er. The determined experimental parameters are compared with theoretical values and the other available experimental values. The results in the present paper are found to be in good agreement with theoretical values and the other results obtained from literature.

## 2. Experimental Procedure

The experimental arrangement is shown in Fig. 1.

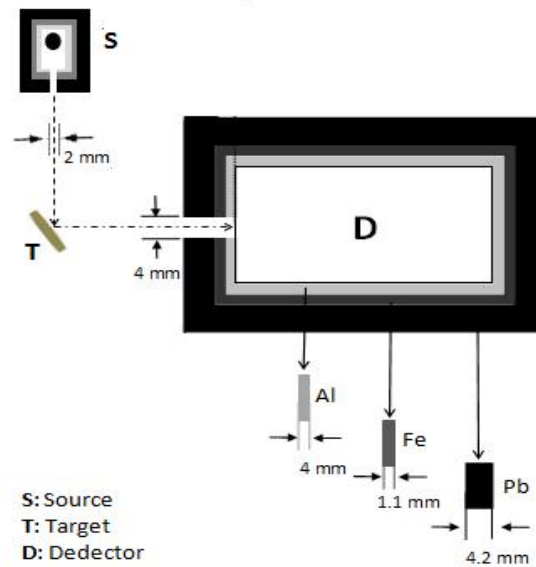


**Figure 1.** Experimental set-up.

The samples were excited using photons of 59.54 keV emitted from Am-241 (about 100 mCi) point source. Spectroscopically pure circular disc (diameter=13 mm) targets of Zr, Mo, Cd and Er of thicknesses ranging from 0.26 to 0.33 g/cm<sup>2</sup> have been used for measurements. The K X-rays were detected by a Si(Li) detector (active area 12 mm<sup>2</sup>, sensitive depth 3 mm, thickness of Be window 0.025 mm and energy resolution of 185 eV at 5.9 keV). The detector was also placed in a step-down shield made from Pb, Fe and Al to minimize the detection of any radiation coming directly from the source and scattered from the surroundings. The spectra were accumulated in time intervals from 3600 to 14400 s in order to obtain sufficient statistical accuracy. In this study, peak integrals were analyzed by using Microcal Origin 7.0 software demo program with least squares fit method. The net peak areas were separated by fitting the measured spectra with multi-Gaussian function plus polynomial backgrounds. Fig. 2 shows a typical K X-rays spectrum for the Er target at 59.54 keV excitation energy.

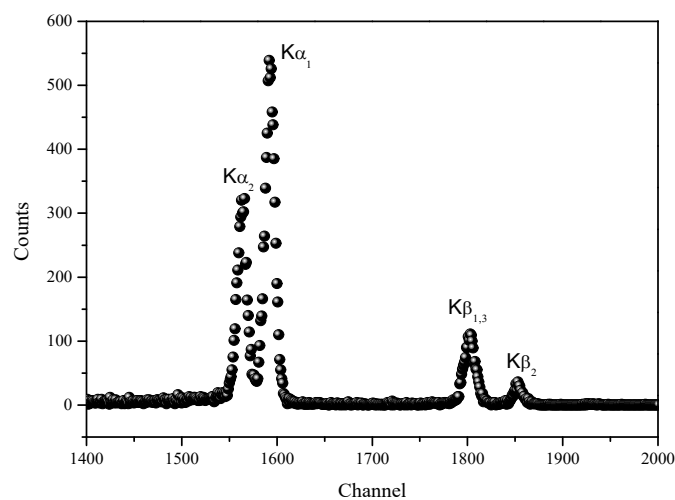


**Figure 2.** Typical K X-ray spectrum for Er at 59.54 keV.

### 3. Experimental and Calculation Procedures

The values of experimental K X-ray fluorescence cross-sections were determined using the following equation:

$$\sigma_{Ki} = \frac{N_{Ki}}{I_0 G \varepsilon_{Ki} \beta_{Ki} t} \quad (i=\alpha, \beta) \quad (1)$$

where  $N_{Ki}$  is the number of counts per second under the corresponding  $K_i$ X-ray photopeak,  $I_0$  is the intensity of the exciting radiation,  $G$  is the geometrical factor dependent on the source-sample-detector geometry,  $\varepsilon_{Ki}$  is the detector efficiency for  $K_i$ X-rays,  $t$  is the thickness of target in g/cm<sup>2</sup> unit and  $\beta_{Ki}$  is the self-absorption correction factor for the target material and is given by:

$$\beta_{Ki} = \frac{1 - \exp[-(\mu_i / \cos \theta_i + \mu_e / \cos \theta_e) t]}{(\mu_i / \cos \theta_i + \mu_e / \cos \theta_e) t} \quad (2)$$

where  $\mu_i$  and  $\mu_e$  are the total mass absorption coefficients of the target material at the incident photon (59.54 keV) and emitted  $K_i$  X-ray energies, respectively. The values of  $\mu_i$  and  $\mu_e$  were taken from WinXCom program [20] being a Windows version of XCOM[21] on the basis of mixture rule. The angles of  $\theta_i$  and  $\theta_e$  which correspond incident and emission angles with sample surface were set to 45°, respectively.

The detector efficiency  $I_0 G \varepsilon_{Ki}$ , which contain terms related to the incident photon flux, geometrical factor and the efficiency of the X-ray detector was determined by measuring  $t$ ;  $\beta_{Ki}$  and the K X-ray intensities from samples of Ti, Cr, Ni, Ru, Ag, Sn, Ce, Pr, Gd, Tb and Ho and using theoretical  $\sigma_{Ki}$  values:

$$I_0 G \varepsilon_{Ki} = \frac{N_{Ki}}{\sigma_{Ki} \beta_{Ki} t} \quad (i=\alpha, \beta) \quad (3)$$

where  $N_{Ki}$  is the number of counts per second under the corresponding  $K_i$  X-ray photopeak,  $\sigma_{Ki}$  is the fluorescence cross sections.

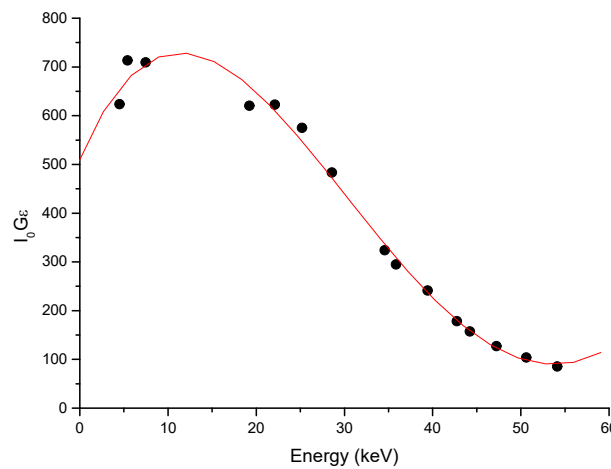


**Figure 3.**  $I_0 G \varepsilon$  values as a function mean K X-ray energy (keV).

The theoretical values of  $\sigma_{Ki}$  fluorescence cross sections were calculated using the following equation:

$$\sigma_{Ki} = \sigma_K(E) \omega_K F_{Ki} \quad (4)$$

where  $\sigma_K(E)$  is the K-shell photoionization cross section taken from Scofield [22] for the elements at the excitation energy,  $\omega_K$  is the K-shell fluorescence yield taken from Krause [1] and  $F_{Ki}$  is the fractional ratio of the  $K_i$  X-rays and  $F_{K\alpha}$  and  $F_{K\beta}$  are defined as:

$$F_{K\alpha} = \left(1 + \frac{I_{K\beta}}{I_{K\alpha}}\right)^{-1} \quad (5)$$

$$F_{K\beta} = \left(1 + \frac{I_{K\alpha}}{I_{K\beta}}\right)^{-1} \quad (6)$$

where  $I_{K\alpha}$  and  $I_{K\beta}$  are the  $K\alpha$  and  $K\beta$  X-ray intensities, respectively. The theoretical values of  $I_{K\beta}/I_{K\alpha}$  were taken from Scofield [23]. The measured  $I_0 G_{E_{Ki}}$  values for the present geometry were plotted as a function of the average K X-ray energy in Fig. 3.

The experimental Kshell fluorescence yields were obtained from using the following expression:

$$\omega_K = \frac{\sum \sigma_{Ki}}{\sigma_K(E)} (i=\alpha, \beta) \quad (7)$$

where  $\sum \sigma_{Ki}$  is the total K X-ray fluorescence cross-section obtained experimentally,  $\sigma_K(E)$  is the theoretical K-shell photoionization cross-section of a given element for the excitation energy taken from Scofield [22].

The experimental K shell level widths were evaluated from the following equation:

$$\Gamma_K = \frac{\Gamma_K(R)}{\omega_K} \quad (8)$$

where  $\Gamma_K(R)$  is radiative transition rate (Scofield, [23]),  $\omega_K$  is the K shell fluorescence yield obtained experimentally.

Experimental radiative vacancy transition probabilities from K shell to  $L_2$ ,  $L_3$ ,  $M_2$  and  $M_3$  sub-shell were investigated from following equation:

$$\eta_{XiYi}(R) = \frac{\Gamma_{XiYi}(R)}{\Gamma_K} \quad (9)$$

$\Gamma_{XiYi}(R)$  is the partial radiative transition rate and taken from Scofield [23],  $\Gamma_K$  is the K shell level width obtained experimentally.

#### 4. Result and Discussion

K shell fluorescence cross sections from eq. 1 for Zr, Mo, Cd, Er at 59,54 keV excitation energy are listed in Table 1 along with the theoretical calculations (eq. 4) by using photoionization cross section (Scofield, [22]), fluorescence yield (Krause, [1]) and fractional emission rates in eqs. (5) and (6). The unit of all cross sections is barns/atom. It is seen from Table 1 that the experimental values are

generally agreement with theoretical predictions within experimental errors (the range  $< 5.7\%$ ,  $< 16.5\%$ ,  $< 4.9\%$ , respectively). The errors are attributed to uncertainties in different parameters used to evaluate K X-ray fluorescence cross sections, namely, the evaluation of peak areas ( $\leq 4.6\%$ ),  $I_0G\epsilon(\leq 5.4\%)$ , thickness ( $\approx 2\%$ ) and absorption correction factor ( $\approx 2\%$ ).

**Table 1.** Experimental and theoretical  $K_i$  ( $i = \alpha, \beta$ , total) X-ray fluorescence cross sections (barns/atom) values.

Element	$\sigma_{K\alpha}$		$\sigma_{K\beta}$		$\sigma_{Ktotal}$	
	Experimental	Theoretical	Experimental	Theoretical	Experimental	Theoretical
$^{40}\text{Zr}$	293.89 $\pm$ 16.52	291.22	57.08 $\pm$ 3.28	50.58	350.96 $\pm$ 27.89	341.80
$^{42}\text{Mo}$	371.90 $\pm$ 20.81	365.37	74.41 $\pm$ 4.27	66.10	446.31 $\pm$ 35.46	431.47
$^{48}\text{Cd}$	682.70 $\pm$ 37.71	650.94	135.67 $\pm$ 8.80	129.86	818.37 $\pm$ 69.94	780.81
$^{68}\text{Er}$	2434.32 $\pm$ 140.60	2303.17	476.18 $\pm$ 31.96	570.26	2910.50 $\pm$ 277.61	2873.43

K shell fluorescence yields and level widths are given in Table 2 with the theoretical results. The unit of all level widths is eV. As seen from Table 2, the agreement of K shell fluorescence yield ( $\omega_K$ ) between the present results and theoretical predictions of Krause [1] are within the range  $< 4.8\%$ . The agreement of level widths between the measured values and theoretical predictions ([9], [10]) are  $< 7.6\%$ ,  $\leq 8.1\%$  for K shell, respectively. As seen from Table 2, the measured  $\omega_K$  and  $\Gamma_K$  values increase with increasing atomic number. The error in  $\omega_K$  and  $\Gamma_K$  values is less than  $< 9.4\%$  for all targets and it mainly arises from the experimental errors in K shell X-ray fluorescence cross sections. The present results are generally in good agreement with other theoretical predictions and theoretical values present in the literature.

**Table 2.** Experimental and theoretical K shell X-ray fluorescence yields ( $\omega_K$ ) and level widths ( $\Gamma_K$ ) values.

Element	$\omega_K$		$\Gamma_K$ (eV)	
	Experimental	Theoretical	Experimental	Theoretical
$^{40}\text{Zr}$	0.749 $\pm$ 0.060	0.730 [1]	3.59 $\pm$ 0.28	3.84[9] 3.83[10]
$^{42}\text{Mo}$	0.791 $\pm$ 0.063	0.765[1]	4.21 $\pm$ 0.33	4.52[9] 4.52[10]
$^{48}\text{Cd}$	0.883 $\pm$ 0.075	0.843[1]	6.73 $\pm$ 0.57	7.28[9] 7.32[10]
$^{68}\text{Er}$	0.959 $\pm$ 0.086	0.947[1]	27.39 $\pm$ 2.61	28.4[9] 28.5[10]

For the measured and calculated radiative vacancy transfer probabilities, eq. (9) were used to include partial radiative transition rates (Scofield, [23]) and level widths from Table 2. The experimental values of K to  $L_2$ ,  $L_3$ ,  $M_2$ ,  $M_3$  radiative vacancy transfer probability are compared with the calculated values from Krause and Oliver [9] and Campbell and Papp [10] in Table 3. The agreement of radiative vacancy transfer probabilities between the measured values and theoretical predictions from [9], [10] are  $< 8.5\%$ ,  $\leq 9\%$  for K shell, respectively.

**Table 3.** Experimental and theoretical K shell to L<sub>2</sub>, L<sub>3</sub>, M<sub>2</sub>, M<sub>3</sub> sub-shells radiative vacancy transfer probability values.

Element	$\eta_{KL2}(R)$		$\eta_{KL3}(R)$	
	Experimental	Theoretical	Experimental	Theoretical
<sup>40</sup> Zr	0.219±0.017	0.205 <sup>a</sup> 0.205 <sup>b</sup>	0.419±0.033	0.392 <sup>a</sup> 0.393 <sup>b</sup>
<sup>42</sup> Mo	0.230±0.018	0.215 <sup>a</sup> 0.215 <sup>b</sup>	0.439±0.035	0.409 <sup>a</sup> 0.409 <sup>b</sup>
<sup>48</sup> Cd	0.256±0.022	0.236 <sup>a</sup> 0.235 <sup>b</sup>	0.480±0.041	0.444 <sup>a</sup> 0.441 <sup>b</sup>
<sup>68</sup> Er	0.277±0.026	0.267 <sup>a</sup> 0.266 <sup>b</sup>	0.492±0.047	0.474 <sup>a</sup> 0.473 <sup>b</sup>
Element	$\eta_{KM2}(R)$		$\eta_{KM3}(R)$	
	Experimental	Theoretical	Experimental	Theoretical
<sup>40</sup> Zr	0.0330±0.0026	0.0309 <sup>a</sup> 0.0310 <sup>b</sup>	0.0644±0.0051	0.0602 <sup>a</sup> 0.0603 <sup>b</sup>
<sup>42</sup> Mo	0.0358±0.0028	0.0333 <sup>a</sup> 0.0333 <sup>b</sup>	0.0696±0.0055	0.0648 <sup>a</sup> 0.0648 <sup>b</sup>
<sup>48</sup> Cd	0.0424±0.0036	0.0392 <sup>a</sup> 0.0390 <sup>b</sup>	0.0824±0.0070	0.0761 <sup>a</sup> 0.0757 <sup>b</sup>
<sup>68</sup> Er	0.0512±0.0049	0.0494 <sup>a</sup> 0.0492 <sup>b</sup>	0.0990±0.0094	0.0955 <sup>a</sup> 0.0952 <sup>b</sup>

<sup>a</sup>Theoretical calculation of radiative vacancy transfer probability from eq. (9) obtained theoretical level widths from Krause and Oliver [9]

<sup>b</sup>Theoretical calculation of radiative vacancy transfer probability from eq. (9) obtained theoretical level widths from Campbell and Papp [10]

The present results are generally in the good agreement with theoretical prediction and other experimental results can be obtained from literature. In order to have a further check for the accuracy and reliability of measured values, more experimental data are needed. The present results confirm the XRF method is simple, direct and fast and reliable way acquiring information on elemental analysis.

## References

- [1] MOKrause and JPhys1979Chem. Ref. Data**8** pp 307
- [2] RYilmaz, HTunç and AÖzkartal2015Radiat. Phys. Chem.**112** pp 83
- [3] ÖŞimşek, ODoğan, ÜTurgut and MErtugrul2000Radiat. Phys. Chem.**58** pp 207
- [4] RDurak and YÖzdemir2001Radiat. Phys. Chem.**61**pp 19
- [5] IHan, MŞahin, LDemir and YŞahin2007Appl. Radiat. Isot.**65** pp 669
- [6] FAKman, RDurak, MRKaçal and MFTurhan2015Can. J. Phys. **93** pp 1057
- [7] SBGudennavar, NMBadiger, SRThontadarya and BHanumaiah2003Radiat. Phys. Chem.**68** pp 721
- [8] RDurak1998Physica Scripta.**58** pp 111
- [9] MOKrause and JHOLiver1979 J. Phys. Chem. Ref. Data **83**pp 329
- [10] JL Campbell, T Papp2001 At. Data Nucl. Data Tables **77** pp 1
- [11] ECengiz, E Tıraşoğlu, G Apaydın, V Aylıkçı, N Küp Aylıkçı and CAksoy2011Radiat. Phys. Chem.**80** pp 328
- [12] MErtugrul2002 J. Anal. At. Spectrom.**17** pp 400

- [13] M Ertuğrul 2002 *Anal. Chem. Acta* **454** pp 327
- [14] F Akman 2016 *Appl. Radiat. Isot.* **115** pp 295
- [15] AS Bennal, KM Niranjan and NM Badiger 2010 *J. Quant. Spectrosc. Radiat. Transfer* **11** pp 1363
- [16] J Reyes-Herrera, J Miranda 2008 *Nucl. Instrum. Methods Phys. Res., Sect. B* **266** pp 5075
- [17] E V Bonzi 2006 *Nucl. Instrum. Methods Phys. Res., Sect. B* **245** pp 363
- [18] F Tuzluca, Ö Söğüt, E Büyükkasap, B G Durdu and A Küçükönder 2008 *Radiat. Phys. Chem.* **77** pp 996
- [19] M F Turhan, R Durak and F Akman 2014 *Appl. Radiat. Isot.* **89** pp 151
- [20] L Gerward, N Guilbert, K B Jensen and H Leving 2001 *Radiat. Phys. Chem.* **60** pp 23
- [21] M J Berger, J H Hubbell, S M Seltzer, J S Coursey and D S Zucker 1998 *NYST Stand. Ref. Database* 8 (XGAM)
- [22] J H Scofield 1973 *Theoretical Report no. UCRL. Lawrence Livermore Laboratory, Livermore, CA* p. 51326
- [23] J H Scofield 1974 *At. Data Nucl. Data Tables* **14** pp 121